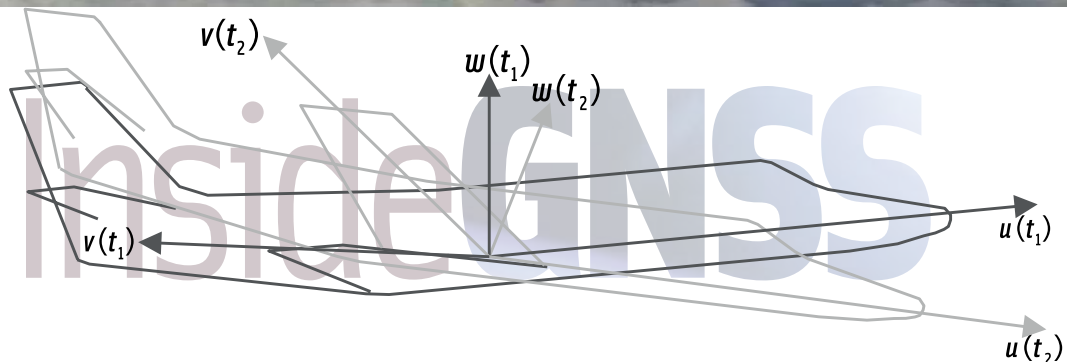
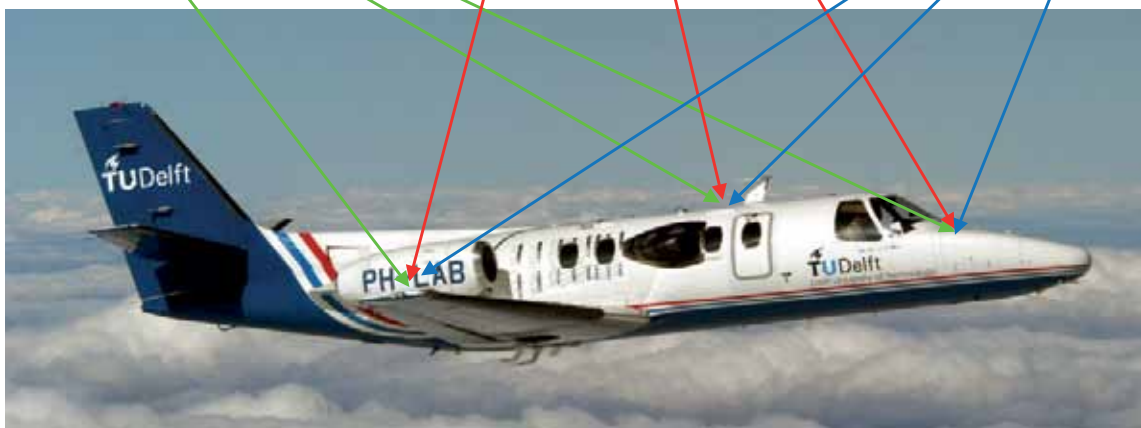


GNSS-Based Attitude Determination

Aerospace and Formation Flying



This article explores the viability of attitude estimation using a GNSS receiver capable of tracking carrier phase signals to precisely estimate a platform's orientation. It introduces a new ambiguity-attitude estimator, in which the two estimation problems—ambiguity resolution and attitude estimation—are coupled and resolved in an integral manner. The authors test the method and apply it to the challenge of flying multiple platforms in formation using relative positioning between the platforms.

GABRIELE GIORGI, PETER J. BUIST, SANDRA VERHAGEN
DELFT UNIVERSITY OF TECHNOLOGY

PETER J.G. TEUNISSEN
CURTIN UNIVERSITY OF TECHNOLOGY, AND DELFT UNIVERSITY OF TECHNOLOGY

Two or more GNSS antennas mounted on one platform may be used as a viable attitude-sensing tool. Although less precise than other sensors, GNSS-based attitude determination is relatively inexpensive and, most importantly, drift-free, unlike inertial sensors.

The orientation of a body with respect to a given reference frame can be estimated by employing two or more antennas. Precise baseline estimates are made available by processing incoming GNSS signals. These can be directly translated into angular estimations of attitude, the accuracy of which depends primarily on two factors: GNSS observation quality and the length of baselines between antennas on a platform. Often one has no control over the latter, because the size and geometry of the platform limit the maximum distance at which the antennas can be placed. Thus, the challenge of obtaining precise angular estimates relies on observation accuracy.

Although GNSS code observations may be used to derive an attitude solution, we generally prefer not to rely solely on these measurements, because for most applications code-based accuracy is inadequate. Alternatively, carrier phase-based position solutions are two orders of magnitude more accurate; however, exploiting carrier phase observations is not a trivial problem.

Only the fractional part of the incoming GNSS phase signal can be detected, making the phase ambiguous by an integer number of full cycles. Correct integer values must be determined by resolving these ambiguities in order to use the carrier phase observations in the attitude estimation process.

Figure 1 illustrates the large difference that occurs between code-based, or *float*, and carrier phase-based, or *fixed*, attitude solutions using a two-meter static baseline. Only the *fixed* phase-based solution is capable of sub-degree accurate angular estimations, an improvement of two orders of magnitude compared to the *float* solution.

Given a matrix of baseline coordinates B and a matrix of local baseline coordinates F relative to the platform, estimating the platform attitude is found using the orthonormal rotation matrix R that transforms B into F , with $B = RF$. This general formulation applies to any attitude sensor that relies on baseline observations to derive the platform orientation.

GNSS-based attitude estimation is based on the same working principle: processing code and phase observations to yield baseline estimates, which are then used to estimate the attitude angles. However, instead of using the traditional sequential approach that de-couples ambiguity resolution and attitude determination into two steps, we formulate the estimation problem in order to solve the integer and attitude estimation problems in an integral manner.

To do this, we first formulate the proper functional GNSS attitude model, as will be shown in the following section, then solve it with a new attitude-ambiguity estimation procedure, using the principles of *Integer Least Squares* (ILS). The method solves for the integer ambiguities by including the whole set of geometric constraints relative to the local baseline frame. In this way we can achieve a significant improvement in ambiguity resolution performance, although at a computational price: this *constrained* ILS method is inherently more complex than *unconstrained* ILS implementations, such as the popular Least-squares AMBiguity Decorrelation Adjustment (LAMBDA) method.

In order to reduce the ILS method's computational expense, we have developed efficient and numerically fast search algorithms to search for the integer minimizer. We will present results from two flight tests and compare the capability of both the unconstrained LAMBDA and the MC-LAMBDA attitude determination methods.

This novel formulation of the attitude-ambiguity estimation problem can be used to enhance relative positioning solutions, of particular importance for formation flying applications. We discuss these results in the final section.

The GNSS Attitude Model

We cast the set of double-difference (DD) GNSS code and phase observations obtained by tracking $n + 1$ satellites on a single frequency into a linear(ized) model,

$$E(y) = Az + Gb; z \in \mathbf{Z}^n, b \in \mathbf{R}^3 \quad (1)$$

$$D(y) = Q_{yy}$$

where, $E(\cdot)$ is the expectation operator, y is the vector of DD code and phase observations, z is the vector containing the n unknown integer-valued ambiguities, and b is the vector of real-valued baseline coordinates. We limit our treatment to single-epoch scenarios.

For attitude determination applications, the distance between antennas is usually limited to few meters, and rarely exceeds tens of meters. In this case, we may disregard all the

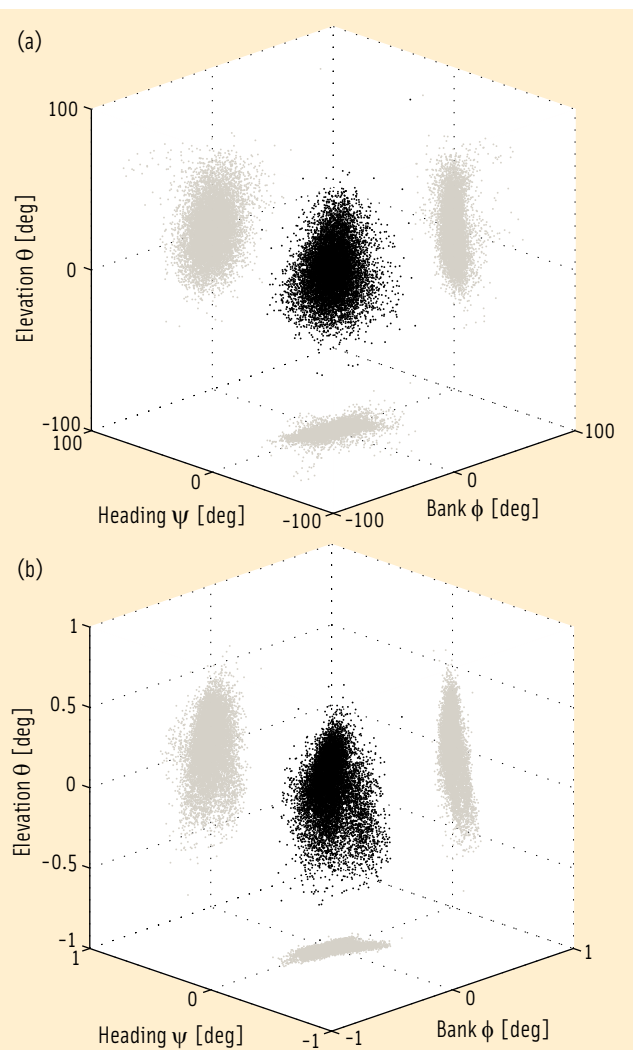


FIGURE 1 Heading, bank and elevation angles of an actual platform carrying two perpendicular two meter-long baselines. The attitude solutions are shown for both the derived, or *float*, measurements (top), as well as the carrier phase-based, or *fixed*, measurements obtained after having correctly resolved the integer ambiguities (bottom). Precision differs between the methods by two orders of magnitude. Gray dots represent the two-dimensional projections on each of the three coordinate planes.

atmospheric delays, which are cancelled by the differencing operations. The only real-valued unknowns are thus the baseline coordinates.

The relationship between code and phase observables, y , and the two vectors of unknowns is given by the matrices A , a $2n \times n$ matrix containing the carrier wavelength, and G , a $2n \times 3$ matrix of DD unit line-of-sight vectors.

We assume a Gaussian noise distribution for the collected observables, whose dispersion $D(y)$ is characterized by the variance-covariance (v-c) matrix Q_{yy} . The integer nature of the ambiguities is given explicitly through the notation $z \in \mathbf{Z}^n$, whereas the baseline vector belongs to the space of real vectors, $b \in \mathbf{R}^3$. Model (1) can be extended for arrays of, say, $m + 1$ antennas. So, the multi-baseline model becomes,

$$E(Y) = AZ + GB; Z \in \mathbf{Z}^{n \times m}, B \in \mathbf{R}^{3 \times m} \tag{2}$$

$$D(\text{vec}(Y)) = Q_{YY}$$

where Y is the $2n \times m$ matrix whose columns are the linearized DD code and phase observations at each baseline, Z is the $n \times m$ matrix whose columns are the integer-valued ambiguity vectors at each baseline, and B is the $3 \times m$ matrix whose columns are the real-valued baseline coordinates. The matrix Q_{YY} describes the dispersion of the vector of observables $\text{vec}(Y)$, where vec is the operator that stacks the columns of a matrix.

One way to derive the attitude of the platform is to solve for the unknowns in model (2), and then estimate the rotation matrix which transforms the baseline matrix B into the local (body-frame) baseline coordinates F . This is the classical approach used in many GNSS-based attitude algorithms available in the literature.

However, we can significantly improve this approach by including the attitude determination problem from the start. We replace the matrix of unknown baseline coordinates B by the unknown rotation matrix R , following the transformation $B = RF$. The resulting GNSS attitude model is

$$E(Y) = AZ + GRF; Z \in \mathbf{Z}^{n \times m}, R \in \mathbf{O}^{3 \times 3} \tag{3}$$

$$D(\text{vec}(Y)) = Q_{YY}$$

where the rotation matrix belongs to the class of 3×3 orthonormal matrices $\mathbf{O}^{3 \times 3}$ for which $R^T R = I_3$. The single-epoch model (3) is much stronger than model (2), by virtue of the additional geometrical constraints.

Multivariate Constrained Integer Least Squares

The GNSS attitude model (3) can be solved in the context of the ILS theory. The solution follows two steps: float estimation and attitude-ambiguity estimation. The float solution is the least-squares solution of (3), in which all the constraints are neglected. This solution is obtained as

$$\begin{pmatrix} \hat{Z} \\ \hat{R} \end{pmatrix} = N^{-1} \begin{bmatrix} I_m \otimes A^T \\ F \otimes G^T \end{bmatrix} Q_{YY}^{-1} \text{vec}(Y) \tag{4}$$

$$N = \begin{bmatrix} I_m \otimes A^T \\ F \otimes G^T \end{bmatrix} Q_{YY}^{-1} \begin{bmatrix} I_m \otimes A & F^T \otimes G \end{bmatrix}$$

The v-c matrix associated with the float solution is obtained by inverting the normal matrix N . The float estimations \hat{Z} and \hat{R} are driven by the precision of the code observables, and thus are not very precise.

In their text, *GPS for Geodesy* (cited in Additional Resources), P. J. G. Teunissen and A. Kleusberg demonstrated that by using the float solution as the initial step, that minimizing the Q_{YY} -weighted, squared norm of residuals in (3) is equal to minimizing the sum-of-squares, thus:

$$\begin{aligned} \{\tilde{Z}, \tilde{R}\} &= \arg \min_{Z \in \mathbf{Z}^{n \times m}, R \in \mathbf{O}^{3 \times 3}} \left\| \text{vec}(Y - AZ - GRF) \right\|_{Q_{YY}}^2 \tag{5} \\ &= \arg \min_{Z \in \mathbf{Z}^{n \times m}} \left[\underbrace{\left\| \text{vec}(\hat{Z} - Z) \right\|_{Q_{ZZ}}^2}_{C(Z)} + \min_{R \in \mathbf{O}^{3 \times 3}} \left\| \text{vec}(\hat{R}(Z) - R) \right\|_{Q_{\hat{R}(Z)\hat{R}(Z)}}^2 \right] \end{aligned}$$

with the notation $\|\cdot\|_Q^2 = (\cdot)^T Q^{-1} (\cdot)$

The constrained ILS Equation (5), with the new ambiguity objective function $C(Z)$, is the minimization problem to be solved. In the unconstrained ILS theory, real-valued unknowns are not constrained, and the last term on the right-hand side of (5) can always be made zero by taking $R = \hat{R}(Z)$ for any integer ambiguity matrix. The solution then becomes the integer matrix that minimizes the squared weighted norm $\left\| \text{vec}(\hat{Z} - Z) \right\|_{Q_{ZZ}}^2$

However, this cannot be applied to the constrained approach in which the sought attitude matrix R must be orthonormal. The minimization problem of Equation (5) is more complicated to solve than the unconstrained version. However, by relying on a much stronger underlying model, the constrained method is capable of improving the ambiguity solution rate.

No analytical solutions for integer minimization problems, such as appear in (5), are known. The ambiguity matrix has to be numerically determined from the set of admissible integer candidates, where

$$\Omega(\chi^2) = \{ Z \in \mathbf{Z}^{n \times m} \mid C(Z) \leq \chi^2 \} \tag{6}$$

The size of the set is defined by the scalar χ^2 , whose value should be small enough to limit the computational burden but still be large enough to guarantee the non-emptiness of $\Omega(\chi^2)$.

For unconstrained problems we can assign a proper value relatively easily to χ^2 by making use of a bootstrapped integer solution. Integer bootstrapping uses covariance information from the float ambiguity covariance matrix to sequentially round the float ambiguities.

For the constrained approach this turns out to be much more challenging because of the very large weighting of the second norm in $C(Z)$. As the precision of $\hat{R}(Z)$ is governed by the very precise phase measurements, the entries of v-c matrix $Q_{\hat{R}(Z)\hat{R}(Z)}$ are much smaller than those of Q_{ZZ} . Therefore, the second term in $C(Z)$ is weighted more heavily than its first term, and consequently,

$$\chi^2 = \left\| \text{vec}(\hat{Z} - Z) \right\|_{Q_{ZZ}}^2 + \min_{R \in \mathbf{O}^{3 \times 3}} \left\| \text{vec}(\hat{R}(Z) - R) \right\|_{Q_{\hat{R}(Z)\hat{R}(Z)}}^2 \gg \left\| \text{vec}(\hat{Z} - Z) \right\|_{Q_{ZZ}}^2 \tag{7}$$

A typical example is given in **Figure 2**. The value of χ^2 is calculated from an integer bootstrapped matrix Z_{boot} for the second flight test described later on. The scalar $\chi^2 = C(Z_{boot})$ is visualized and compared with the value

$$\chi_1^2 = \left\| \text{vec}(\hat{Z} - Z_{boot}) \right\|_{Q_{zz}}^2$$

Their four-order difference in magnitude is due to the difference in magnitude between the phase-variance and code-variance.

This large difference in magnitude is the main difficulty that arises when searching for the integer minimizer, \tilde{Z} , of $C(Z)$. The evaluation of the cost function $C(Z)$ involves the solution of a constrained least-squares problem to extract the orthonormal matrix R . If the number of candidates for which this has to be done exceeds a reasonable value, the search becomes too time-consuming and impractical.

In order to overcome this difficulty, we introduce the Multivariate Constrained LAMBDA (MC-LAMBDA) method, which modifies the popular LAMBDA method to tackle constrained ILS problems such as (5).

MC-LAMBDA: Fast Implementation of Constrained ILS

We devised a fast numerical approach for solving Equation (5) based on the LAMBDA method by exploiting two properties of the cost functions.

First, similar to what is done in the standard, unconstrained LAMBDA method, the ambiguities are decorrelated. This partially mitigates “halting” problems, by reducing the set of independent integer ambiguities which are not contained in the search space, given any initial set of independent integer ambiguities.

Then, in place of the extensive search algorithm, we implement an alternative method based on approximating functions

that are easier to evaluate than $C(Z)$. We define two bounding functions using the smallest (λ_{\min}) and largest (λ_{\max}) eigenvalues of $Q_{\hat{R}(Z)\hat{R}(Z)}$:

$$C_1(Z) = \left\| \text{vec}(\hat{Z} - Z) \right\|_{Q_{zz}}^2 + \lambda_{\min} \sum_{i=1}^3 \left(\|\hat{r}_i(Z)\|_l - 1 \right)^2 \quad (8)$$

$$C_2(Z) = \left\| \text{vec}(\hat{Z} - Z) \right\|_{Q_{zz}}^2 + \lambda_{\max} \sum_{i=1}^3 \left(\|\hat{r}_i(Z)\|_l + 1 \right)^2$$

where $\hat{r}_i(Z)$ is the i -th column of $\hat{R}(Z)$ and the inequalities are derived from the rules of the scalar product between vectors.

Based on these bounding functions, we devise two efficient search strategies for the constrained ILS minimization, the *expansion* approach and the *search and shrink* approach. The first approach works by enumerating all the integer matrices contained in a small set of admissible candidates and iteratively increasing the search space until the minimizer is found.

The search and shrink approach takes the opposite approach: it starts from a large set and proceeds by iteratively shrinking the size of the search space until one candidate is found, namely, the minimizer.

The two search strategies provide an efficient method for identifying the integer minimizer, by fixing the initial size of the search space and speeding up the search by avoiding the computation of the constrained LS problem a large number of times. The cost function $C(Z)$ is then evaluated only for a small set of integer candidates.

This solution achieves a proper use of the bounding functions $C_1(Z)$ and $C_2(Z)$. Further improvements could be obtained by employing tighter bounding functions.

A Comparison of Attitude Estimation Algorithms

Given an integer matrix of ambiguities, Z , we estimate the platform attitude by solving the constrained LS problem

$$\tilde{R}(Z) = \min_{R \in O^{3,3}} \left\| \text{vec}(\hat{R}(Z) - R) \right\|_{Q_{\hat{R}(Z)\hat{R}(Z)}}^2 \quad (9)$$

where, $\tilde{R}(Z)$ is the orthonormal matrix obtained by projecting the data vector $\text{vec}(\hat{R}(Z))$ onto the multi-dimensional curved manifold defined by the geometric constraints of the normality and orthogonality of the columns of R . We need to be able to extract the solution of (9) in a timely manner, in order to reduce the overall computational time of the ambiguity search.

An analytical solution to Equation (9) has been known since the 1960s only for a diagonal matrix $Q_{\hat{R}(Z)\hat{R}(Z)}$, a case known as Wahba’s problem. Various numerically efficient methods have been proposed to solve for Wahba’s problem, such as the Quaternion ESTimator (QUEST), the Fast Optimal Attitude Matrix (FOAM), the EStima-

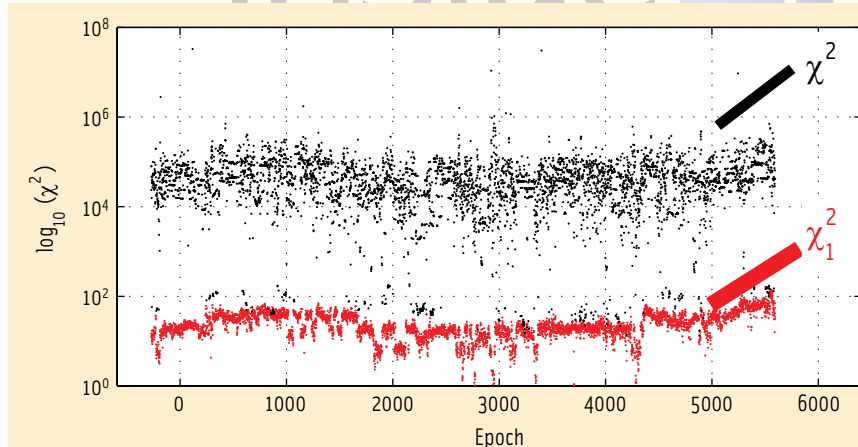


FIGURE 2 Demonstration of the large values of χ^2 in Equation (7). The value $\chi^2 = C(Z_{boot})$ is a few orders of magnitude larger than

$$\chi_1^2 = \left\| \text{vec}(\hat{Z} - Z_{boot}) \right\|_{Q_{zz}}^2$$

for the same bootstrapped integer matrix Z_{boot}

tor of the Optimal Quaternion (ESOQ) or the Second ESOQ (ESOQ2) algorithms.

Although fast, these methods only *approximate* a solution to Equation (9) when the matrix $Q_{\hat{R}(Z)\hat{R}(Z)}$ is fully populated. Hence, in order to rigorously solve the nonlinear LS problem Equation (9), we need to employ alternative methods. Three examples of such methods are:

(a) the Lagrangian Multiplier Method, which aims to find the stationary points of the Lagrangian function,

$$L(R, [\mu]) = \left\| \text{vec} \left(\hat{R}(Z) - R \right) \right\|_{Q_{\hat{R}(Z)\hat{R}(Z)}}^2 - \text{tr} \left([\mu] R^T R - I_3 \right) \quad (10)$$

where $[\mu]$ is the 3×3 symmetric matrix of Lagrangian multipliers.

(b) the Euler Angle Method, which re-parameterizes the attitude matrix in terms of the vector of Euler angles ε , and applies Newton's iteration method to find the minimizer of the (unconstrained) nonlinear LS problem,

$$\min \left\| \text{vec} \left(\hat{R}(Z) - R(\varepsilon) \right) \right\|_{Q_{\hat{R}(Z)\hat{R}(Z)}}^2 \quad (11)$$

(c) the Quaternion Method, which re-parameterizes the attitude matrix in terms of quaternions, \bar{q} , and solves for the stationary points of the Lagrangian function,

$$L(R(\bar{q}), \mu) = \left\| \text{vec} \left(\hat{R}(Z) - R(\bar{q}) \right) \right\|_{Q_{\hat{R}(Z)\hat{R}(Z)}}^2 - \mu \left(\bar{q}^T \bar{q} - 1 \right) \quad (12)$$

Methods (a), (b) and (c) rigorously solve Equation (9), but are generally slower than the approximated methods, SVD,

EIG, QUEST, FOAM, ESOQ, and ESOQ2. **Figure 3** illustrates the simulation results obtained by comparing the approximated methods with the iterative algorithms (a), (b) and (c), in terms of floating-point operations and processing time. The latter is given only to compare the relative performance between approaches. The absolute values may vary largely depending on hardware and implementation.

The approximation techniques outperform the iteration techniques because the number of required floating-point operations in the former is two to three orders of magnitude lower.

Among the second set of methods, the Lagrangian multiplier technique generally requires the highest number of operations, making it the least efficient method, while the Euler angle method and the Quaternion parameterization provide better overall results. **Figure 4** shows the corresponding mean, maximum and minimum computational times marked during the simulations. The Lagrangian parameterization method generally takes the longest time to converge, whereas the quaternion and Euler angle methods show better results. Note that higher number of floating operations does not directly translate into longer computational times, because modern processor architectures efficiently operate by means of multi-threading and parallel processing.

Application Example: Aircraft Attitude Determination

The newly developed MC-LAMBDA method is being tested on a wide range of platforms, while varying antennas/receivers grade, constellation availability and quality, and platform dynamics. The most interesting test results obtained to this date have been from applying this method to data collected on a flying platform.

Several flight tests have been performed aboard the Cessna Citation II PH-LAB. This is an aircraft owned and operated jointly by the Delft University of Technology (DUT) and the Dutch Nationaal Lucht-en Ruimtevaartlaboratorium (NLR, National Aerospace Laboratory) that is equipped with various test systems and facilities, including a selection of GPS antennas.

The first flight analyzed took place on June 2, 2005, in the north of The Netherlands, using a single GNSS receiver connected to three antennas: one placed on the

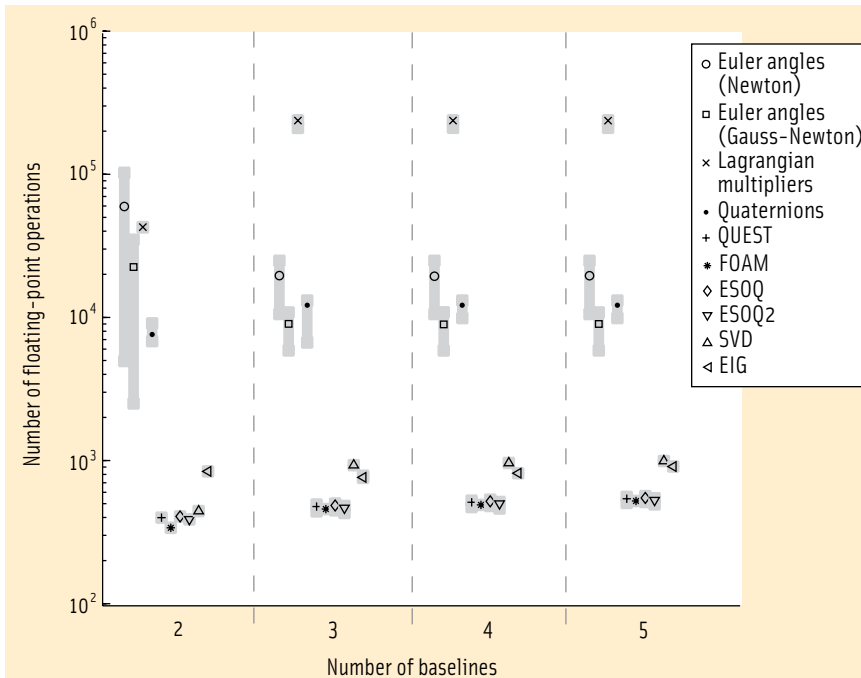


FIGURE 3 Mean number of floating-point operations for different attitude estimation methods, per number of baselines (or number of antennas+1) employed. The gray bars span between the maximum and minimum numbers obtained for each algorithm. 10^4 course solutions generated via Monte Carlo simulations.

	Unaided, single-frequency, single-epoch success rate [%]
LAMBDA	5.8
MC-LAMBDA	81.5

TABLE 1. First flight test. The unaided single-epoch, single-frequency success rate (%) for the LAMBDA and MC-LAMBDA methods.

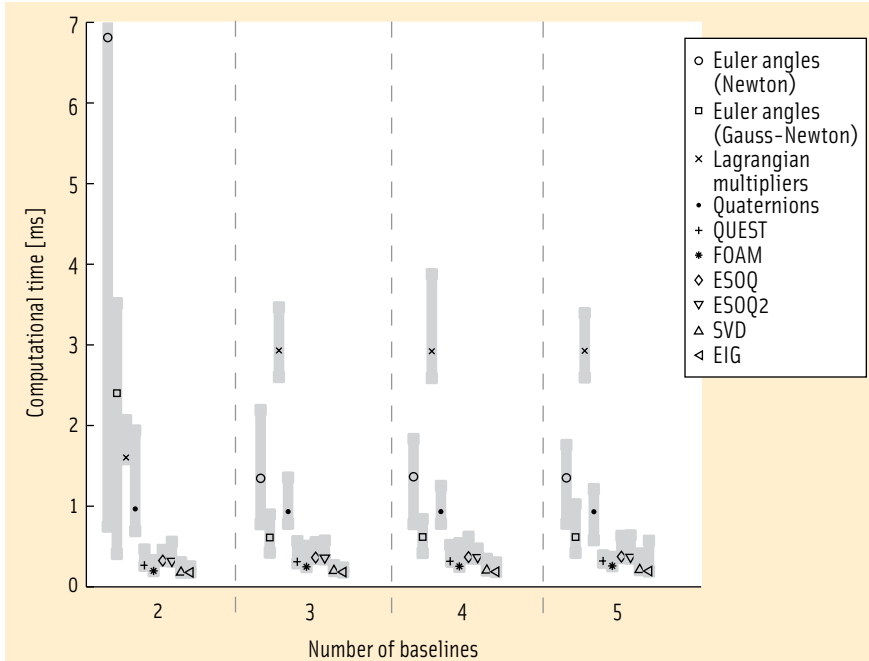


FIGURE 4 Mean computational time marked by the different attitude estimation methods, per number of baselines (or number of antennas+1) employed. The gray bars span between the maximum and minimum numbers obtained for each algorithm. 10^4 course solutions generated via Monte Carlo simulations.

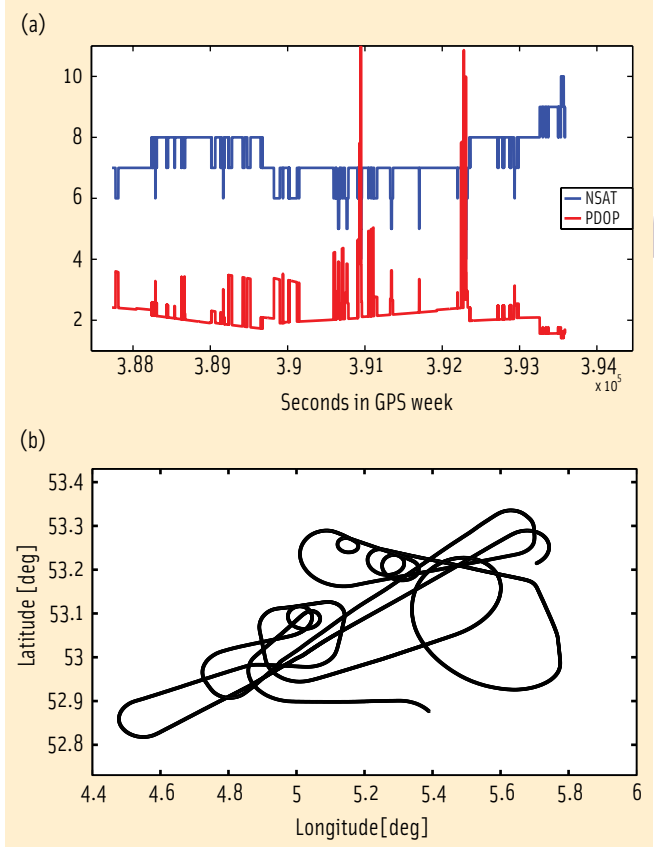


FIGURE 5 First flight test: number of common satellites tracked and PDOP values (top) and ground track (bottom)

middle of the fuselage, and two L1 antennas — one placed at the end of the left wing and the other on a boom on the nose. The receiver logged one-hertz data during the flight test, between 11:42 and 13:20 UTC (Coordinated Universal Time). The number of tracked satellites, PDOP, and horizontal trajectory of the flight (ground track) are shown in **Figure 5**. The data was then processed with both the unconstrained LAMBDA and MC-LAMBDA methods, and the single-frequency, single-epoch success rates obtained are reported in **Table 1**.

In computations using the collected data, the LAMBDA method was unable to provide correct integer ambiguities from a single-epoch set of observations more than 5.8 percent of the time, whereas the MC-LAMBDA method largely improves the fixing rate, with 81.5 percent of the epochs correctly resolved, thus providing a reliable epoch-by-epoch attitude solution for the largest part of the flight.

During the flight the pilot performed a variety of maneuvers, such as a zero-gravity arc, where the aircraft pitched up then quickly down to create a virtual absence of gravity on board. This maneuver was perfectly tracked epoch-by-epoch with the MC-LAMBDA method, as shown in **Figure 6**.

A second test flight was performed in the context of an airborne remote sensing campaign, the Gravimetry using Airborne Inertial Navigation (GAIN) project. The same configuration of the receiver and three antennas was duplicated, except that the antenna was mounted directly on the nose, instead of a boom.

The receiver logged data for the entire duration of the flight, from 10:06 to 14:18 UTC. The number of available satellites, PDOP values, and the flight ground track are shown in **Figure 7**. To support the gravimetry campaign, a high-precision inertial navigation system/inertial reference system (INS/IRS) was also

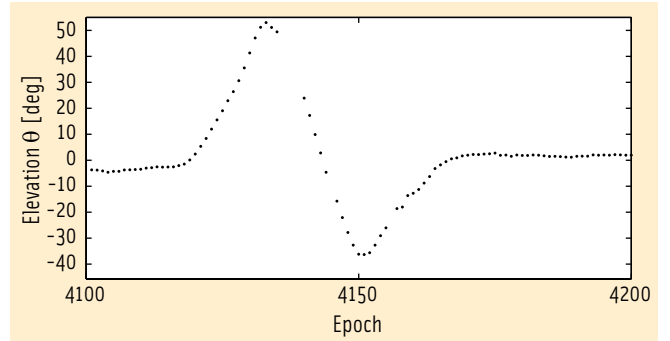


FIGURE 6 First flight test. The zero-gravity maneuver is tracked epoch-by-epoch with the MC-LAMBDA method. Only in five epochs was the correct ambiguity matrix not found.

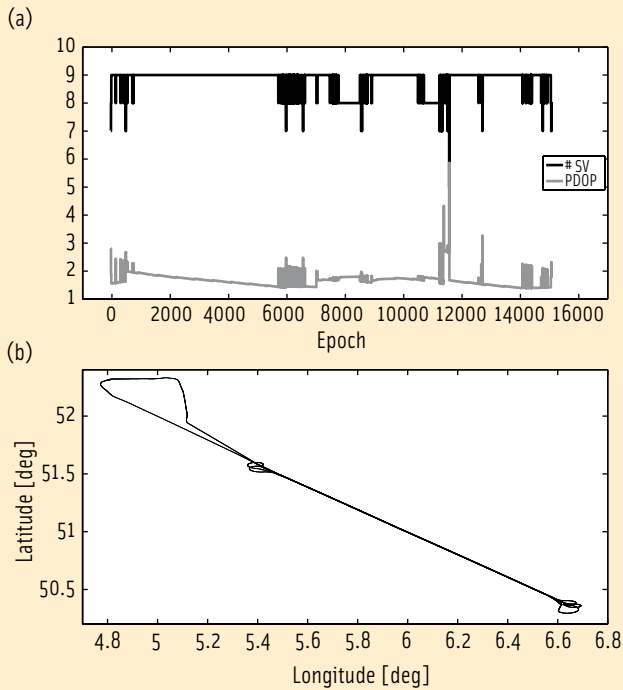


FIGURE 7 Second flight test. Top: number of common satellites tracked and PDOP values. Bottom: Ground track

carried on board, allowing for a comparison of the INS attitude solutions with those generated by GNSS.

The unaided, single-frequency, single-epoch success rates for the LAMBDA and MC-LAMBDA methods are reported in Table 2. The higher number of satellites available during the second flight test helped to improve the performance of the unconstrained methods.

The LAMBDA method was capable of fixing the correct set of integer ambiguities 40.3 percent of the time — much higher than in the first flight test but still insufficient to be a reliable method on a single-epoch basis. Comparatively, the MC-LAMBDA method again demonstrated a very large improvement, providing the correct integer matrix for more than 95 percent of the epochs. Hence, the precise attitude solution was available for the largest part of the flight duration. Figure 8 shows the attitude angles as derived with the GPS observations for the time span considered.

Figure 8 also shows the output of the INS. Standard deviations of the differences between the output of the INS and the GPS-based attitude solution are 0.01 degrees for the heading angle, 0.20 degrees for the elevation angle, and 0.12 degrees for the bank angle. The heading angle is estimated with the highest precision, whereas the elevation shows the highest noise levels. The bank angle estimation is more accurate than the elevation one, being driven by the longer baseline formed by the antennas on the nose and on the wing.

Attitude-Bootstrapped Improved Relative Positioning

The MC-LAMBDA method, described in the previous section, can be used in other ways, for example, to improve relative

	Unaided, single-frequency, single-epoch success rate [%]
LAMBDA	40.3
MC-LAMBDA	95.8

TABLE 2. Second flight test. The unaided single-epoch, single-frequency success rate (%) for the LAMBDA and the MC-LAMBDA methods.

positioning in the formation flying.

Traditionally, in multi-platform missions, such as formation flying and rendezvous, the GNSS-based

attitude determination and relative positioning problems are treated independently. Recent research has shown that multi-antenna data can also be used to enhance the relative positioning between the platforms. This approach makes use of an approximation of the ILS by first solving the attitude determination problem for each individual platform with the MC-LAMBDA method and then to use its solution to improve the baseline estimation so that the *bootstrapped* solution can find the baseline between platforms. This integrated approach is coined *attitude-bootstrapped relative positioning*.

In this section we will discuss a case in which two platforms either side of a baseline have the same number of antennas ($m + 1$). C is the total number of independent baselines at both platforms (e.g., $C = 2m$). The most common configuration for GNSS-based attitude determination is the use of three or four antennas on a single platform, but platforms carrying fewer antennas are also used. These scenarios are depicted in Figure 9.

We describe the integrated approach principle by providing an example that demonstrates the improved multi-antenna solution.

First, consider a configuration with a single antenna at each platform ($C = 0$): the variance of the conditional baseline estimate is given as $Q_{b(\varepsilon)b(\varepsilon)}$. Then, with two antennas at each platform ($C = 2$ in Figure 9), the baseline at the first platform is indicated with b_1^1 , the baseline at the second platform is indicated with b_2^2 , and the baselines between the two antennas at each of the two platforms are denoted with b_1^{12} and b_2^{12} . Assuming that the baseline lengths between the antennas at each platform b_1^1 and b_2^2 are precisely known and the ambiguity vectors at these baselines can be determined successfully using the MC-LAMBDA method, the baseline coordinates for each platform can be determined precisely, in the millimeter range.

As a consequence, the baseline between the first two antennas at both platforms can be estimated by either differencing between these antennas, or by estimating the baseline between the remaining two antennas at both platforms and then forming the baseline $b_1^{12} = b_2^{12} + b_1^1 - b_2^2$, where $b_1^1 - b_2^2$ is known precisely. Hence the *same* baseline is observed twice and thus the variance of the baseline estimate is improved by a factor of 0.5.

This discussion can be extended to a larger number of antennas at each of the platforms, and also to the non-symmetric case with a different number of antennas at each platform.

This discussion can be supported by analytical analyses. For the baseline between the platforms the improvement of both ambiguity resolution and baseline precision for the multi-antenna solution can be demonstrated to be a function of the number of antennas at each platform. The ambiguity and

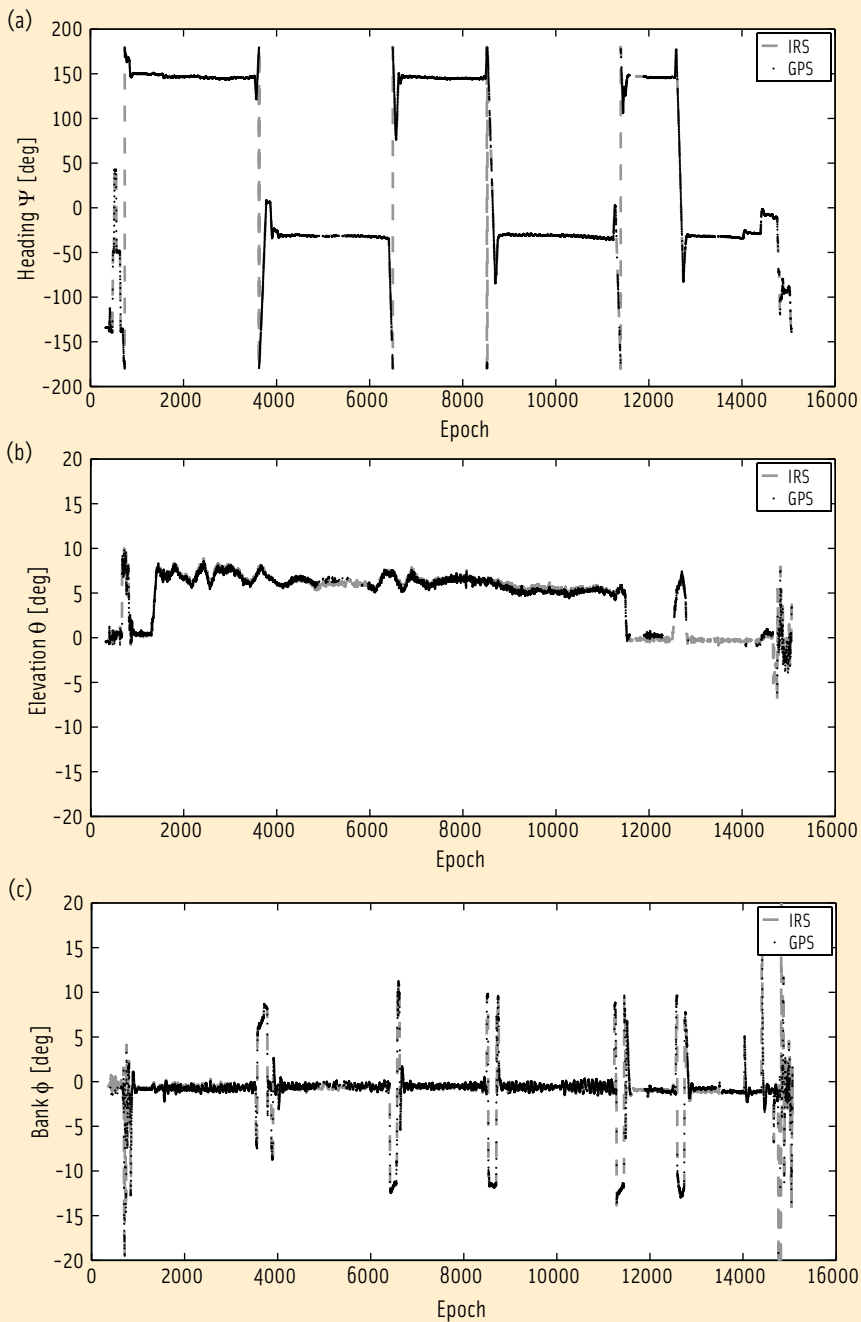


FIGURE 8 Second flight test: The three attitude angles estimated with GNSS signals with precise INS output is plotted as well.

baseline vectors can be estimated with a precision improved by a factor,

$$Q_{Boots} = \frac{1}{1+m} Q \tag{13}$$

where Q_{Boots} is the v-c matrix of the bootstrapped solution. This reduction is important as it will result in higher success rates for ambiguity resolution and more precise baseline estimates. The performance of attitude-bootstrapped

relative positioning has been demonstrated using simulations and data obtained from experiments, found in the Additional Resources section.

Conclusion

We have introduced a new method of GNSS-based attitude determination. Instead of following the classical approach of first estimating the base-

lines from carrier phase observations and then estimating the attitude matrix, the new MC-LAMBDA method has the orthonormal constraints of the attitude matrix incorporated into the ambiguity objective function from the start.

As a result the *a priori* geometric information is properly weighted in the ambiguity objective function and provides guidance for the search of the integer minimizer. The increased complexity is tackled by means of easy-to-use bounding functions, which allow for an efficient and fast numerical solution. By tightening the relation between the attitude and the ambiguity estimation problems, the new method is capable of maximizing the probability of successful integer ambiguity resolution, while making epoch-by-epoch precise attitude solutions available in a timely manner.

The novel ambiguity-attitude estimation method can also be employed to enhance a relative positioning solution between a number of platforms with multiple antennas. When flying multiple platforms in formation, each carrying a number of antennas, reliable ambiguity estimation for the baselines at each platform implies higher redundancy in the inter-platform baseline measurements. This allows for higher probabilities of correctly fixing the ambiguities between the different platforms and more precise baseline estimates.

Acknowledgements

Peter Teunissen is Federation Fellow of the Australian Research Council (project FF0883188). This support is gratefully acknowledged. The research of Sandra Verhagen is supported by the Dutch Technology Foundation STW, applied science division of NWO, and the Technology Program of the Ministry of Economic Affairs. The GAIN experiment team, a mutual cooperation between chairs of Control and Simulation, Physical and Space Geodesy and Mathematical Geodesy and Positioning at TU Delft is acknowledged for the pleasant cooperation during the flight tests. This work is supported by the Australian Space Research Program GARA-DA project on SAR Formation Flying.

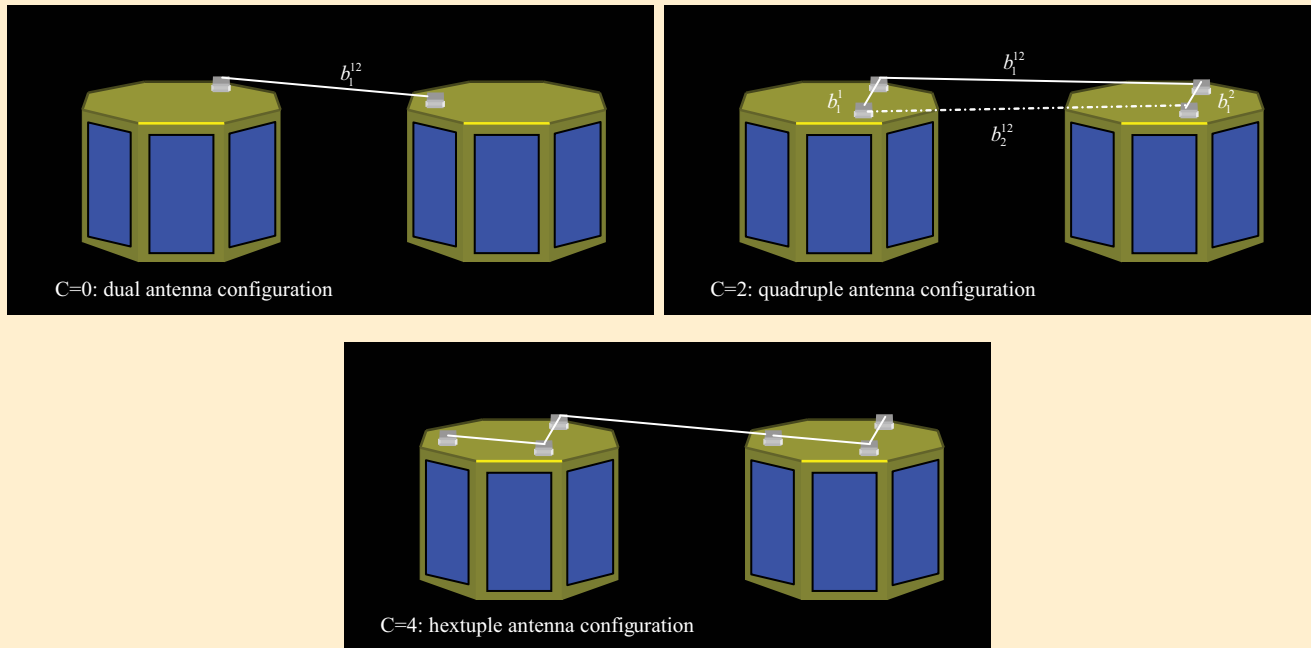


FIGURE 9 Definition of two platforms and C-baseline configuration

Manufacturers

The receiver installed on the aircraft was a PolaRx2@ from **Septentrio nv**, Leuven, Belgium. The AIL DM-C L1-L2 antenna placed on the middle of the fuselage was from **ITT Corporation**, Bohemia, New York, USA. The two L1 antennas placed on the wing and the nose were from **Sensor Systems, Inc.**, Chatsworth, California, USA. The data presented in this article was plotted using MATLAB from **The Mathworks, Inc.** Natick, Massachusetts, USA.

Additional Resources

- [1] Buist, P. J., and P. J. G. Teunissen, G. Giorgi, and S. Verhagen, "Multi-Platform Instantaneous GNSS Ambiguity Resolution for Triple and Quadruple Antenna Configurations with Constraints," *International Journal of Navigation and Observation*, vol. 2009, Article ID565426, doi:10.1155/2009/565426, 2009
- [2] Buist, P.J., P.J.G. Teunissen, G. Giorgi, S. Verhagen, "A Vectorial Bootstrapped Approach for Integrated GNSS-based Relative Positioning and Attitude Determination of Spacecraft," *Acta Astronautica*, 68(7-8): 1113-1125, DOI: 10.1016/j.actaastro.2010.09.027. (2010)
- [3] Buist, P.J., and P.J.G. Teunissen, G. Giorgi, and S. Verhagen, "Multivariate Bootstrapped Relative Positioning of Spacecraft Using GPS L1/Galileo E1 Signals," *Advances in Space Research*, 47(5): 770-

785 *Scientific applications of Galileo and other Global Navigation Satellite Systems - II*, DOI: 10.1016/j.asr.2010.10.001, 2010

- [4] Cheng Y., and M. D. Shuster, "Robustness and Accuracy of the QUEST Algorithm," *Advances in the Astronautical Sciences*, 127:41-61, 2007
- [5] Giorgi, G., and P. J. G. Teunissen, S. Verhagen, and P. J. Buist, "Integer Ambiguity Resolution with Nonlinear Geometrical Constraints", *Proceedings of the VII Hotine-Marussi Symposium on Mathematical Geodesy*, Rome, Italy, 2009
- [6] Giorgi, G., and P. J. G. Teunissen, "Carrier Phase GNSS Attitude Determination with the Multivariate Constrained LAMBDA Method," *Proceedings of the 2010 IEEE-AIAA Aerospace Conference*, Big Sky, Montana, USA, Paper 1103, 2010
- [7] Giorgi, G., and P. J. G. Teunissen, S. Verhagen, and P. J. Buist, "Instantaneous Ambiguity Resolution in GNSS-based Attitude Determination Applications: the MC-LAMBDA Method," *Journal of Guidance, Control and Dynamics*, accepted for publication, April 2011.
- [8] Markley, F. L., and D. Mortari, "How to Estimate Attitude from Vector Observations," presented at AAS/AIAA Astrodynamics Specialist Conference, Paper 99-427, 1999
- [9] Teunissen, P. J. G., and A. Kleusberg, *GPS for Geodesy*, Springer, Berlin Heidelberg New York, 1998
- [10] Teunissen, P. J. G., "Integer Least-Squares Theory for the GNSS Compass," *Journal of Geodesy*, 84(7):433-447, 2010

- [11] Teunissen, P. J. G., and G. Giorgi and P. J. Buist, "Testing of a New Single-Frequency GNSS Carrier-Phase Attitude Determination Method: Land, Ship and Aircraft Experiments," *GPS Solutions*, 15(1):15-28, 2010
- [12] Teunissen, P. J. G., "Mixed Integer Estimation and Validation for Next Generation GNSS," *Handbook of Geomathematics*, Edited by W. Freeden et alia, Part V, 1101-1127, 2010
- [13] Wahba, G. "Problem 65-1: A Least Squares Estimate of Spacecraft Attitude," *SIAM Review*, 7(3): 384-386, 1965

Authors



Gabriele Giorgi is a Ph.D. candidate at the Mathematical Geodesy and Positioning (MGP) section, Delft Institute of Earth Observation and Space Systems (DEOS),

Delft University of Technology, in Delft, The Netherlands. His main research focuses on attitude determination with next-generation GNSS. He has an M.Sc. degree in space engineering from the University of Rome "La Sapienza" and a B.Sc. degree in aerospace engineering from the same university.

Peter Buist is a GNSS researcher at Delft University of Technology (DUT). He received his master degree in the field of aerospace engineering from DUT. After eight years in the Japanese industry working on GNSS applications for space, Buist



returned to Delft. Currently he is working on integrated attitude determination and relative positioning for formation flying in the GARADA project.



Peter J. G. Teunissen is a professor of geodesy and Earth observation, Federation Fellow of the Australian Research Council (ARC), and Positioning Science Director

of the Cooperative Research Centre for Spatial Information (CRC-SI). His current research focus is on modeling next-generation GNSS for high-accuracy relative navigation and attitude determination in space and air. He is the inventor of the LAMBDA method and has more than 25 years of GNSS research experience.



Sandra Verhagen obtained her Ph.D. from Delft University of Technology (DUT) and is now an assistant professor there. Her research

focuses on ambiguity resolution and integrity monitoring for real-time kinematic GNSS applications, for which she received a research grant from the Dutch Science Organization (NWO). She is president of the Commission for Positioning and Application of the International Association of Geodesy (IAG).



Guenter W. Hein serves as the editor of the Working Papers column. He is head of the Galileo Operations and Evolution Department of the European Space Agency. Previously, he was a full professor and director of the Institute of Geodesy and Navigation at the University FAF Munich. In 2002 he received the prestigious Johannes Kepler Award from the U.S. Institute of Navigation (ION) for "sustained and significant contributions to satellite navigation." He is one of the CBOC inventors. [IG](#)

He is one of the CBOC inventors. [IG](#)

E-News from **InsideGNSS**

SIGNALS

An Electronic Newsletter for the GNSS Community

Monthly reportage and analysis providing a top-level perspective on the world's GNSS programs, policies, and technology



For your free subscription, sign up online at www.insidegnss.com/eneews

To advertise, contact richard@insidegnss.com